SUPPLEMENTARY MATERIAL

Identification of potential cytotoxic inhibitors from *Physalis minima*

Le Canh Viet Cuong[a], Le Ba Vinh[e,g], Pham Thi Hai Yen[a,b], Le Thi Lien[a,b], Pham Thi Thuy Hoai[a], Ton That Huu Dat[a], Do Thi Thao[c], Bach Long Giang[d], Young Ho Kim[g,*], Hoang Le Tuan Anh[a,b,*]

[a] *Mientrung Institute for Scientific Research, Vietnam Academy of Science and Technology (VAST), 321 Huynh Thuc Khang street, Hue city, Vietnam*

[b] *Graduate University of Science and Technology, VAST, 18 Hoang Quoc Viet street, Hanoi city, Vietnam*

[c] *Institute of Biotechnology, VAST, 18 Hoang Quoc Viet street, Hanoi city, Vietnam*

[d] *Nguyen Tat Thanh University, 300A Nguyen Tat Thanh street, Ho Chi Minh city, Vietnam*

[e] *Institute of Marine Biochemistry, VAST, 18 Hoang Quoc Viet street, Hanoi city, Vietnam*

[g] *Chungnam National University, Daejeon, 34134, Republic of Korea*

* **To whom correspondence should be addressed**:

Hoang Le Tuan Anh, PhD, Email: hoangletuananh.misr@gmail.com

Young Ho Kim, PhD/Prof, Email: yhk@cnu.ac.kr

Abstract

A phytochemical investigation of *Physalis minima* led to the isolation of six withanolides, including withanolide E (**1**), withaperuvin C (**2**), 4*β*-hydroxywithanolide E (**3**), 28-hydroxywithaperuvin C (**4**), physaperuvin G (**5**), and 4-deoxywithaperuvin (**6**). Their chemical structures were elucidated by 1D-NMR and 2D-NMR data, as well as comparison with the data reported in the literature. All isolated compounds were evaluated for their cytotoxic activity against HepG2, SK-LU-1, and MCF7 cancer cell lines. As the obtained results, compounds **1** and **3** displayed the strongest cytotoxicity against HepG2, SK-LU-1, and MCF7 cell lines with IC_{50} value ranging from 0.051 ± 0.004 to 0.86 ± 0.09 μg/mL.

Keywords: *Physalis minima, withanolide, anti-cancer, cytotoxic activity.*

CONTENTS

General experimental procedures

The NMR spectra were measured on Bruker AM500 MHz spectrometers with TMS as an internal standard. Column chromatography (CC) was performed on silica gel (Kiesel gel 60, 70-230 mesh and 230-400 mesh, Merck, Darmstadt, Germany), YMC*GEL (ODS-A, 12 nm S-150 μm, YMC Co., Ltd.) and Sephadex LH-20 (Sigma-Aldrich, USA) resins. TLC used pre-coated silica gel 60 F_{254} (1.05554.0001, Merck) and RP-18 F_{254S} plated (1.15685.0001, Merck), and compounds were visualized by spraying aqueous 10% H_2SO_4 by heating. Solvents and standard were purchased from Sigma Aldrich.

Cell lines and cell culture

The SK-LU-1 **(**human lung carcinoma), HepG2 (human hepatocellular carcinoma), and MCF7 (human breast carcinoma) cell lines were a generous gift from Dr. J. M. Pezzuto, University of Long Island, USA and Dr. Jeanette Maier, Università degli Studi di Milano, Italy.

The cells were cultured as a monolayer in Dulbeco's Modified Eagle Medium (DMEM) containing 2 mM L-glutamine, 1.5 g/L sodium bicarbonate, 4.5 g/L glucose, 10 mM HEPES, 1.0 mM sodium pyruvate, and 10% Fetal Bovine Serum (FBS). The MCF7 medium was further added with 0.01 mg/mL bovine insulin while LNCaP medium was supplemented with 10 nM of testosterone. The cells were subcultured after 3-5 days with the ratio of 1:3 and incubated at 37^{o}C, 5% CO_2 and 100% humidified.

Cytotoxicity assay

Cytotoxic assays were performed according to a method developed by Monks et al, which is being used at the National Institute of Health (USA) as a standard method for the evaluation of the cytotoxic potential of compounds or extracts using a panel of human cancer cell lines (Monks et al. 1991). Cell lines were grown in 96-well microtiter plates with each well containing 190 μl medium. After 24 hrs, 10 μl of the test samples dissolved in 10% DMSO were added to the wells. The cells were then cultured for additional 48 hrs, fixed with trichloroacetic acid, and stained with sulforhodamine B, followed by the determination of the optical densities at 515 nm using an EL× 800 Microplate Reader (Bio-Tek Instruments) (Shoemaker et al. 2002). The inhibitory rate of cell growth (IR) of cells was calculated by the following equation IR = 100% - [(OD_t - OD_0) / (OD_c - OD_0)] x 100, where: OD_t : average OD value at day 3; OD_0: average OD value at time-zero; OD_c: average OD value of the blank DMSO control sample.

The cytotoxicities were calculated and expressed as Inhibition concentration at 50 % (IC_{50} values). The IC_{50} values of promising agents will be determined by testing a series of sample final concentrations at 100, 20, 4, 0.8, 0.16, and 0.032 μg/mL. Experiments were carried out in triplicate

for accuracy of data. The TableCurve 2Dv4 software was used for data analysis and for IC_{50} calculation. The IC_{50} values should be in small deviation throughout the experiments.

Biological materials

The aerial parts of *Physalis minima* L. were collected at Huong Hoa commune, Nam Dong district, Thua Thien Hue province, Vietnam (16º09′40″N 107º41′59″E) in September 2018, and were identified by Ms. Nguyen Quynh Nga (National Institute of Medicinal Materials, Vietnam). The voucher specimen (MISR2018-18) has been deposited at the herbarium of Mientrung Institute for Scientific Research, VAST, Vietnam. The aerial parts of *P. minima* (28.5 kg, fresh) were dried in an air-circulating oven at 40ºC for 7 days, then ground into dried powder (2.6 kg) and subjected to solvent extraction.

Extraction and isolation

The dried and powdered aerial parts of *P. minima* (2.6 kg) were extracted three times (each 5 L) with MeOH by sonication for 2 h. The MeOH extract was concentrated under reduced pressure to obtain a residue (PM, 150.0 g). This residue was suspended in water (1.5 L) and successively partitioned with *n*-hexane (3 × 2 L), dichloromethane (3 × 2 L), and ethyl acetate (3 × 2 L) to give: *n*-hexane (PMH, 31.0 g), dichloromethane (PMD, 15.0 g), ethyl acetate (PME, 8.0 g) and a water layer after removal of the solvents. The PMD fraction was subjected to a silica gel CC and eluted with dichloromethane/methanol (20/1, v/v) to yield three sub-fractions (PMD1-PMD3). The sub-fraction PMD2 was further purified by an RP-18 CC using solvent methanol/water (2/1, v/v) to afford compound **1 (**40 mg). The sub-fraction PMD3 was further separated by a silica gel CC using solvent dichloromethane/methanol, (20/1, v/v) and an RP-18 CC using solvent acetone/water (1/2, v/v) to yield compounds **2** (20 mg) and **3** (50 mg). The PME fraction was subjected to a silica gel CC and eluted with dichloromethane/methanol (20/1, v/v) to yield five sub-fractions (PME1-PME5). The sub-fraction PME3 was purified by a silica gel CC and eluted with dichloromethane/methanol (20/1, v/v) to obtained compound **5** (6 mg). The fraction PME5 was further separated by silica gel CC using solvent dichloromethane/methanol (12/1, v/v) to give compounds **4** (15 mg) and **6** (8 mg).

Spectroscopic data

Withanolide E (**1**): White amorphous powder; ^{1}H-NMR (MeOD-d_4, 500 MHz): δ_H 6.01 (1H, dd, J = 2.5, 10.0 Hz, H-2), 6.98 (1H, ddd, J = 2.5, 6.0, 10.0 Hz, H-3), 1.94 (1H, m, H_a-4), 2.97 (1H, dt, J = 2.5, 18.5 Hz, H_b-4), 3.24 (1H, d, J = 2.0 Hz, H-6), 1.84 (1H, m, H_a-7), 1.94 (1H, m, H_b-7), 1.95 (1H, m, H-8), 1.83 (1H, m, H-9), 1.65 (1H, m, H_a-11), 2.00 (1H, m, H_b-11), 1.55 (1H, m, H_a-12), 1.70 (1H, m, H_b-12), 1.30 (1H, m, H_a-15), 2.28 (1H, m, H_b-15), 1.58 (1H, dd, J = 8.5, 14.0 Hz, H_a-16), 2.58 (1H, m, H_b-16), 1.11 (3H, s, H-18), 1.25 (3H, s, H-19), 1.39 (3H, s, H-21), 4.86 (1H, d, J = 3.5 Hz, H-22), 2.53 (1H, m, H_a-23), 2.66 (1H, dd, J = 3.5, 18.5 Hz, H_b-23), 1.87 (3H, s, H-27), 1.98 (3H,

s, H-28); ^{13}C-NMR (MeOD-d_4, 125 MHz): δ_C 205.4 (C-1), 129.9 (C-2), 146.7 (C-3), 33.7 (C-4), 63.3 (C-5), 65.1 (C-6), 27.5 (C-7), 35.2 (C-8), 38.4 (C-9), 49.8 (C-10), 24.3 (C-11), 33.3 (C-12), 55.6 (C-13), 84.0 (C-14), 31.5 (C-15), 37.4 (C-16), 88.7 (C-17), 21.0 (C-18), 15.1 (C-19), 79.8 (C-20), 19.4 (C-21), 82.9 (C-22), 35.7 (C-23), 153.4 (C-24), 122.0 (C-25), 169.1 (C-26), 12.3 (C-27), 20.5 (C-28).

Withaperuvin C (**2**): White amorphous powder; ^{1}H-NMR (MeOD-d_4, 500 MHz): δ_H 6.00 (1H, d, J = 10.0 Hz, H-2), 7.09 (1H, dd, J = 6.0, 10.0 Hz, H-3), 6.23 (1H, d, J = 6.0 Hz, H-4), 4.60 (1H, t, J = 3.0 Hz, H-6), 1.64 (1H, m, H$_a$-7), 1.95 (1H, dt, J = 3.0, 14.0 Hz, H$_b$-7), 2.47 (1H, m, H-8), 1.80 (1H, m, H-9), 1.67 (1H, m, H$_a$-11), 1.72 (1H, dd, J = 4.5, 12.5 Hz, H$_b$-11), 1.37 (1H, m, H$_a$-12), 2.22 (1H, dd, J = 5.5, 12.0 Hz, H$_b$-12), 1.54 (1H, m, H$_a$-15), 1.82 (1H, m, H$_b$-15), 1.59 (1H, m, H$_a$-16), 2.57 (1H, m, H$_b$-16), 1.21 (3H, s, H-18), 1.49 (3H, s, H-19), 1.39 (3H, s, H-21), 4.83 (1H, m, H-22), 1.54 (1H, m, H$_a$-23), 1.68 (1H, dd, J = 2.5, 18.5 Hz, H$_b$-24), 1.85 (3H, s, H-27), 1.99 (3H, s, H-28); ^{13}C-NMR (MeOD-d_4, 125 MHz): δ_C 208.2 (C-1), 126.7 (C-2), 142.9 (C-3), 118.4 (C-4), 160.4 (C-5), 75.0 (C-6), 37.6 (C-7), 35.8 (C-8), 44.2 (C-9), 55.7 (C-10), 22.6 (C-11), 31.5 (C-12), 55.6 (C-13), 84.7 (C-14), 33.4 (C-15), 37.5 (C-16), 88.5 (C-17), 21.2 (C-18), 18.7 (C-19), 79.8 (C-20), 19.4 (C-21), 82.8 (C-22), 35.7 (C-23), 153.4 (C-24), 121.9 (C-25), 169.0 (C-26), 12.3 (C-27), 20.6 (C-28).

4*β*-Hydroxywithanolide E (**3**): White amorphous powder; ^{1}H-NMR (MeOD-d_4, 500 MHz): δ_H 6.20 (1H, d, J = 10.0 Hz, H-2), 7.07 (1H, dd, J = 6.5, 10.0 Hz, H-3), 3.68 (1H, d, J = 6.5 Hz, H-4), 3.24 (1H, brs, H-6), 1.90 (1H, t-like, J = 12.0 Hz, H$_a$-7), 2.01 (1H, m, H$_b$-7), 1.83 (1H, m, H-8), 1.52 (1H, m, H-9), 1.57 (2H, m, H-11), 1.55 (1H, m, H$_a$-12), 1.72 (1H, td, J = 8.5, 12.0 Hz, H$_b$-12), 1.28 (1H, m, H$_a$-15), 2.23 (1H, td, J = 6.0, 12.0 Hz, H$_b$-15), 1.58 (1H, m, H$_a$-16), 2.56 (1H, m, H$_b$-16), 1.09 (3H, s, H-18), 1.41 (3H, s, H-19), 1.39 (3H, s, H-21), 4.83 (1H, d, J = 3.5 Hz, H-22), 2.54 (1H, m, H$_a$-23), 2.65 (1H, dd, J = 3.0, 8.5 Hz, H$_b$-23), 1.86 (3H, s, H-27), 1.98 (3H, s, H-28); ^{13}C-NMR (MeOD-d_4, 125 MHz): δ_C 204.2 (C-1), 133.4 (C-2), 145.0 (C-3), 71.1 (C-4), 64.8 (C-5), 62.0 (C-6), 27.2 (C-7), 35.3 (C-8), 38.4 (C-9), 49.9 (C-10), 22.2 (C-11), 33.2 (C-12), 55.5 (C-13), 83.8 (C-14), 31.0 (C-15), 37.4 (C-16), 88.6 (C-17), 20.7 (C-18), 16.6 (C-19), 79.8 (C-20), 19.4 (C-21), 82.8 (C-22), 35.6 (C-23), 153.4 (C-24), 121.9 (C-25), 169.1 (C-26), 12.31 (C-27), 20.5 (C-28).

28-Hydroxywithaperuvin C (**4**): White amorphous powder; ^{1}H-NMR (MeOD-d_4, 500 MHz): δ_H 6.00 (1H, d, J = 9.5 Hz, H-2), 7.09 (1H, dd, J = 6.0, 9.5, H-3), 6.23 (1H, d, J = 6.0, H-4), 4.60 (1H, t, J = 3.0, H-6), 1.95 (1H, dt, J = 3.0, 13.5, H$_a$-7), 2.59 (1H, m, H$_b$-7), 2.50 (1H, td, J = 3.0, 16.5, H-8), 1.81 (1H, m, H-9), 1.67 (1H, m, H$_a$-11), 1.72 (1H, m, H$_b$-11), 1.45 (1H, m, H$_a$-12), 2.20 (1H, m, H$_b$-12), 1.55 (1H, dd, J = 3.5, 12.5, H$_a$-15),1.85 (1H, m, H$_b$-15), 1.63 (2H, m, H-16), 1.23 (3H, s, H-18), 1.49 (3H, s, H-19), 1.41 (3H, s, H-21), 4.83 (1H, d, J = 3.5, H-22), 2.41 (1H, m, H$_a$-23), 3.09 (1H, dd, J = 2.5, 18.0, H$_b$-23), 1.87 (3H, s, H-27), 4.19 (1H, d, J = 14.0, H$_a$-28), 4.40 (1H, d, J = 14.0, H$_b$-28); ^{13}C-NMR (MeOD-d_4, 125 MHz): δ_C 208.2 (C-1), 126.7 (C-2), 142.9 (C-3), 118.4 (C-4), 160.5

(C-5), 75.0 (C-6), 37.6 (C-7), 35.8 (C-8), 44.3 (C-9), 55.7 (C-10), 22.6 (C-11), 31.4 (C-12), 55.8 (C-13), 84.8 (C-14), 33.4 (C-15), 37.5 (C-16), 88.6 (C-17), 21.1 (C-18), 18.7 (C-19), 79.9 (C-20), 19.5 (C-21), 83.9 (C-22), 30.5 (C-23), 154.9 (C-24), 122.3 (C-25), 169.1 (C-26), 11.8 (C-27), 61.6 (C-28).

Physaperuvin G (**5**): White amorphous powder; ^{1}H-NMR (MeOD-d_4, 500 MHz): δ_H 5.78 (1H, dd, J = 2.5, 10.0 Hz, H-2), 6.66 (1H, dq, J = 2.0, 10.0 Hz, H-3), 2.06 (1H, dd, J = 5.0, 20.0 Hz, H_a-4), 3.27 (1H, dt, J = 2.5, 20.0 Hz, H_b-4), 3.60 (1H, t, J = 2.5 Hz, H-6), 1.49 (1H, br d, J = 10.0 Hz, H_a-7), 2.12 (1H, dd, J = 3.0, 13.5 Hz, H_b-7), 3.55 (1H, m, H-8), 2.25 (1H, td, J = 4.5, 12.5 Hz, H-9), 1.52 (1H, m, H_a-11), 2.31 (1H, m, H_b-11), 1.31 (1H, m, H_a-12), 2.40 (1H, td, J = 4.5, 12.0 Hz, H_b-12), 1.58 (1H, m, H_a-15), 1.78 (1H, dt, J = 8.5, 13.0 Hz, H_b-15), 1.57 (1H, m, H_a-16), 2.60 (1H, m, H_b-16), 1.17 (3H, s, H-18), 1.34 (3H, s, H-19), 1.40 (3H, s, H-21), 4.90 (1H, dd, J = 3.0, 13.0 Hz, H-22), 2.53 (1H, m, H_a-23), 2.67 (1H, dd, J = 3.0, 18.5 Hz, H_b-23), 1.88 (1H, s, H-27), 1.98 (1H, s, H-28); ^{13}C-NMR (MeOD-d_4, 125 MHz): δ_C 207.5 (C-1), 129.1 (C-2), 143.8 (C-3), 36.7 (C-4), 78.2 (C-5), 75.6 (C-6), 29.9 (C-7), 35.0 (C-8), 35.2 (C-9), 53.4 (C-10), 23.8 (C-11), 32.3 (C-12), 56.0 (C-13), 85.0 (C-14), 33.3 (C-15), 37.4 (C-16), 89.0 (C-17), 21.6 (C-18), 16.1 (C-19), 79.8 (C-20), 19.6 (C-21), 83.2 (C-22), 35.8 (C-23), 153.3 (C-24), 122.0 (C-25), 169.1 (C-26), 12.3 (C-27), 20.5 (C-28);

4-Deoxywithaperuvin (**6**): White amorphous powder; ^{1}H-NMR (MeOD-d_4, 500 MHz): δ_H 5.94 (1H, dd, J = 2.0, 10.0 Hz, H-2), 6.88 (1H, m, H-3), 2.50 (1H, dd, J = 5.5, 20.5 Hz, H_a-4), 2.90 (1H, dt, J = 2.5, 20.5 Hz, H_b-4), 3.85 (1H, dd, J = 5.5, 12.0 Hz, H-6), 1.64 (1H, m, H_a-7), 1.83 (1H, m, H_b-7), 2.01 (1H, td, J = 4.0, 12.0 Hz, H-8), 2.09 (1H, td, J = 5.0, 12.0 Hz, H-9), 0.94 (1H, m, H_a-11), 1.49 (1H, dd, J = 5.0, 13.5 Hz, H_b-11), 1.28 (1H, m, H_a-12), 2.21 (1H, td, J = 5.0, 12.0 Hz, H_b-12), 1.55 (1H, m, H_a-15), 1.78 (1H, dt, J = 8.5, 13.0 Hz, H_b-15), 1.58 (1H, m, H_a-16), 2.58 (1H, dt, J = 3.0, 11.5 Hz, H_b-16), 1.09 (3H, s, H-18), 1.17 (3H, s, H-19), 1.39 (3H, s, H-21), 4.79 (1H, dd, J = 3.5, 13.0 Hz, H-22), 2.54 (1H, m, H_a-23), 2.64 (1H, dd, J = 3.0, 14.0 Hz, H_b-23), 1.83 (3H, s, H-27), 1.96 (3H, s, H-28); ^{13}C-NMR (MeOD-d_4, 125 MHz): δ_C 205.3 (C-1), 127.9 (C-2), 147.0 (C-3), 31.5 (C-4), 79.6 (C-5), 73.3 (C-6), 32.9 (C-7), 38.8 (C-8), 39.1 (C-9), 56.2 (C-10), 24.1 (C-11), 31.4 (C-12), 55.9 (C-13), 84.1 (C-14), 33.1 (C-15), 37.5 (C-16), 88.6 (C-17), 21.2 (C-18), 9.3 (C-19), 79.8 (C-20), 19.4 (C-21), 82.8 (C-22), 35.7 (C-23), 153.4 (C-24), 121.9 (C-25), 169.0 (C-26), 12.3 (C-27), 20.5 (C-28);

Table S1. Cytotoxic activity of compounds **1**-**6**

Compounds	**IC_{50} (µg/mL)**		
	HepG2	**SK-LU-1**	**MCF7**
1	0.051 ± 0.004	0.056 ± 0.003	0.059 ± 0.006
2	19.50 ± 1.75	14.65 ± 0.82	11.74 ± 1.01
3	0.80 ± 0.05	0.86 ± 0.09	0.83 ± 0.13
4	>100	>100	>100
5	>100	>100	>100
6	64.44 ± 3.93	56.22 ± 6.22	65.33 ± 4.06
Ellipticine	0.38± 0.02	0.46± 0.05	0.41±0.03

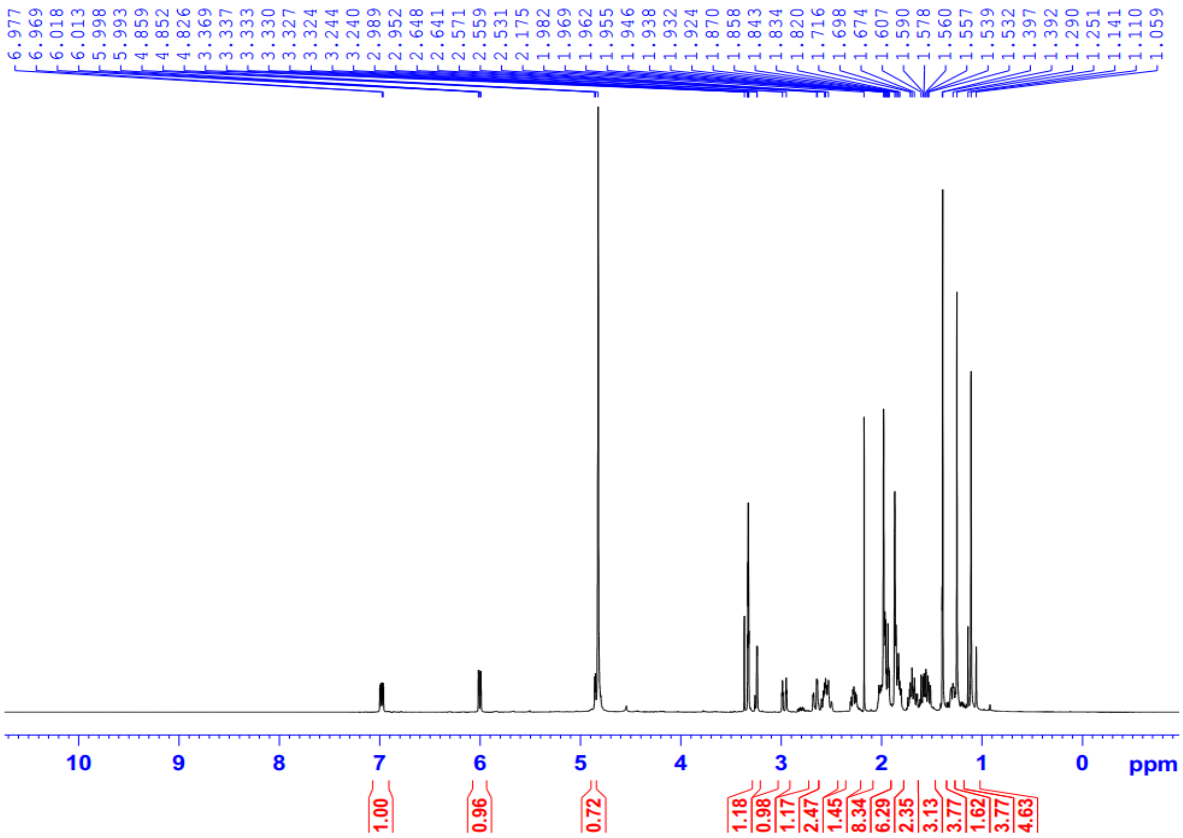

Figure S1. ^{1}H-NMR spectrum (MeOD-d_4, 500 MHz) of compound (**1**)

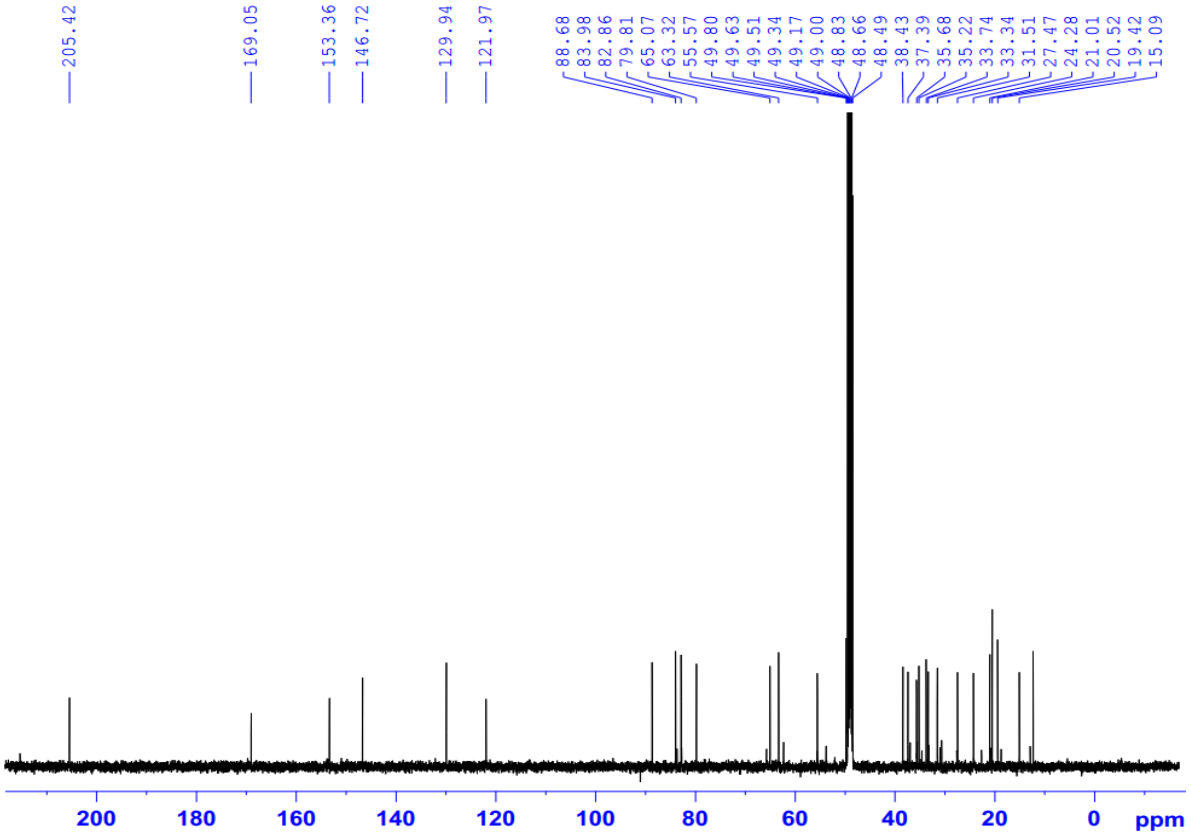

Figure S2. ^{13}C-NMR spectrum (MeOD-d_4, 125 MHz) of compound (**1**)

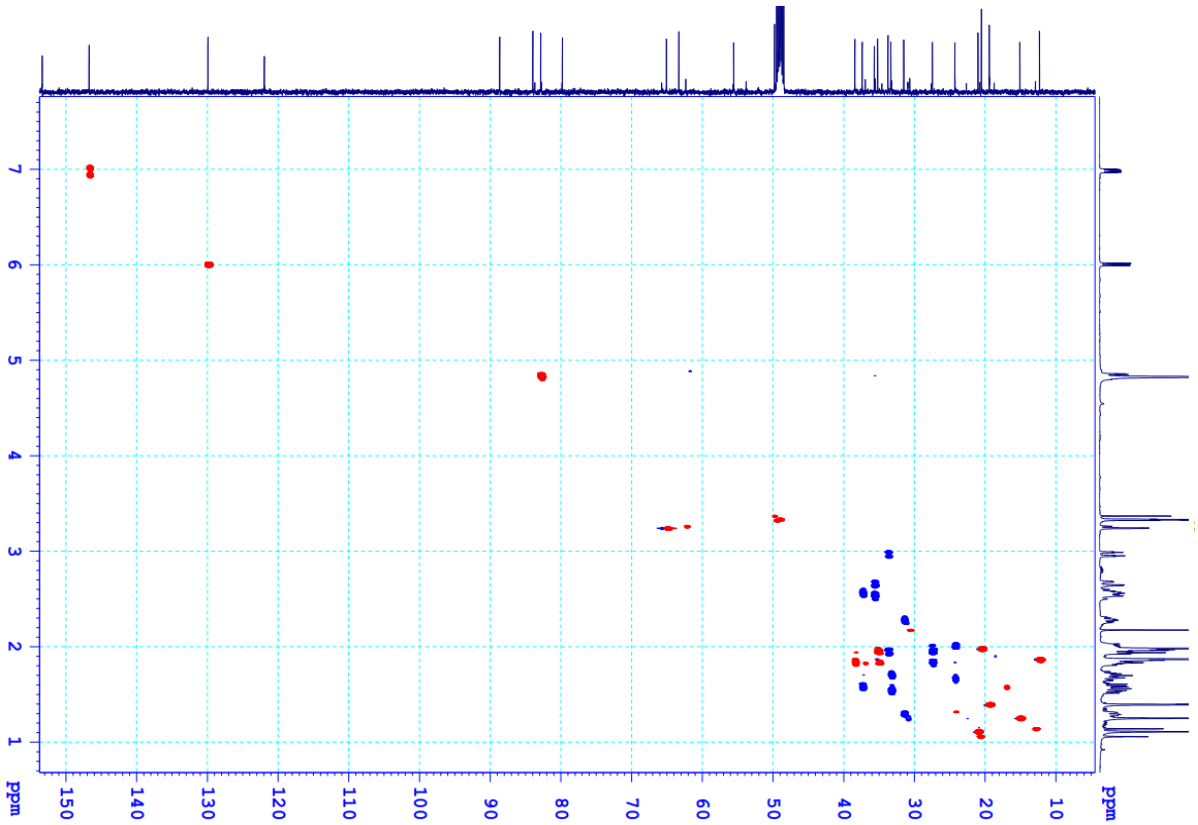

Figure S3. HSQC spectrum of compound (**1**)

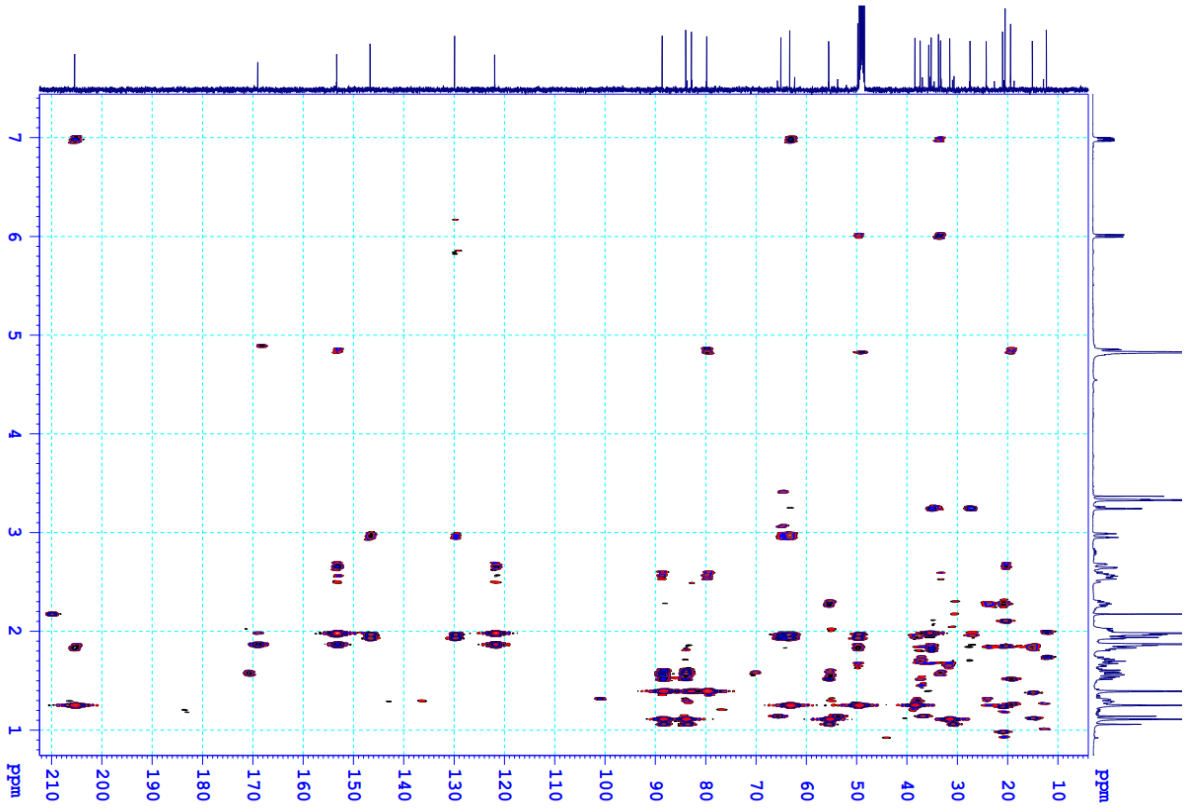

Figure S4. HMBC spectrum of compound (**1**)

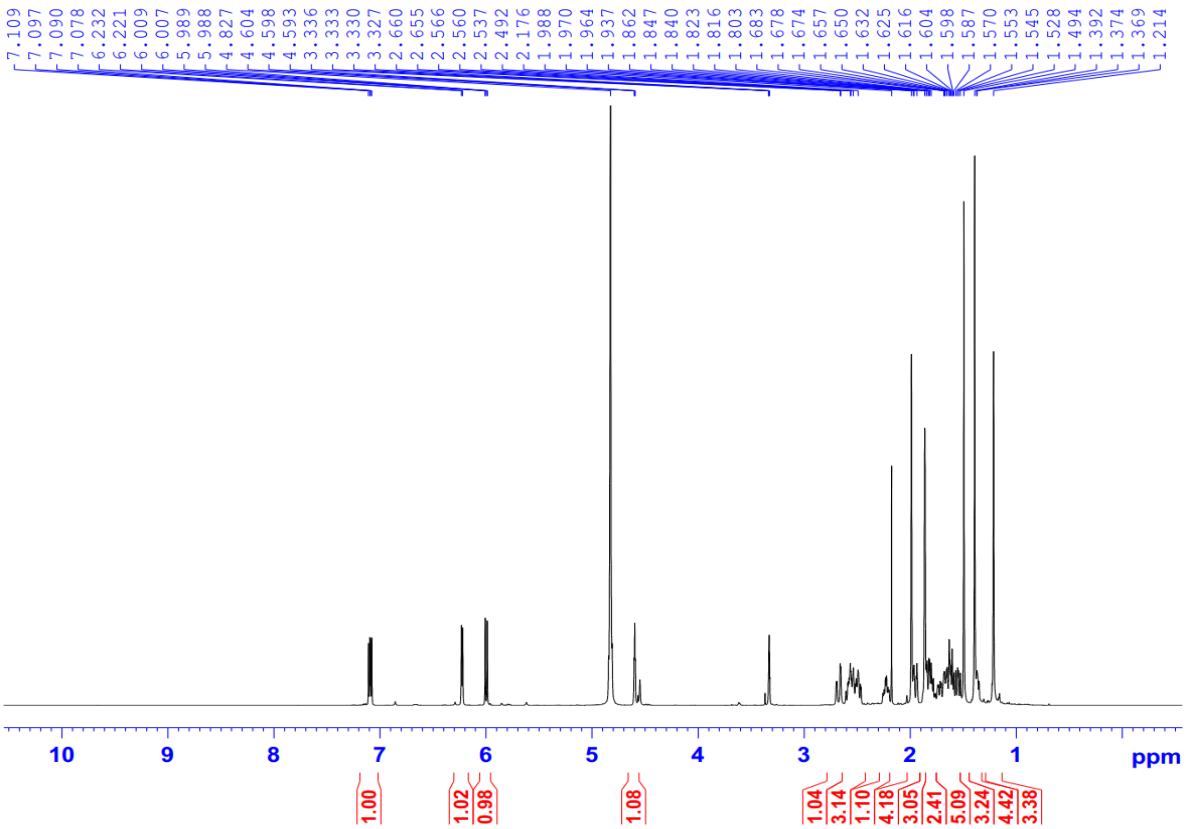

Figure S5. ^{1}H-NMR spectrum (MeOD-d_4, 500 MHz) of compound (**2**)

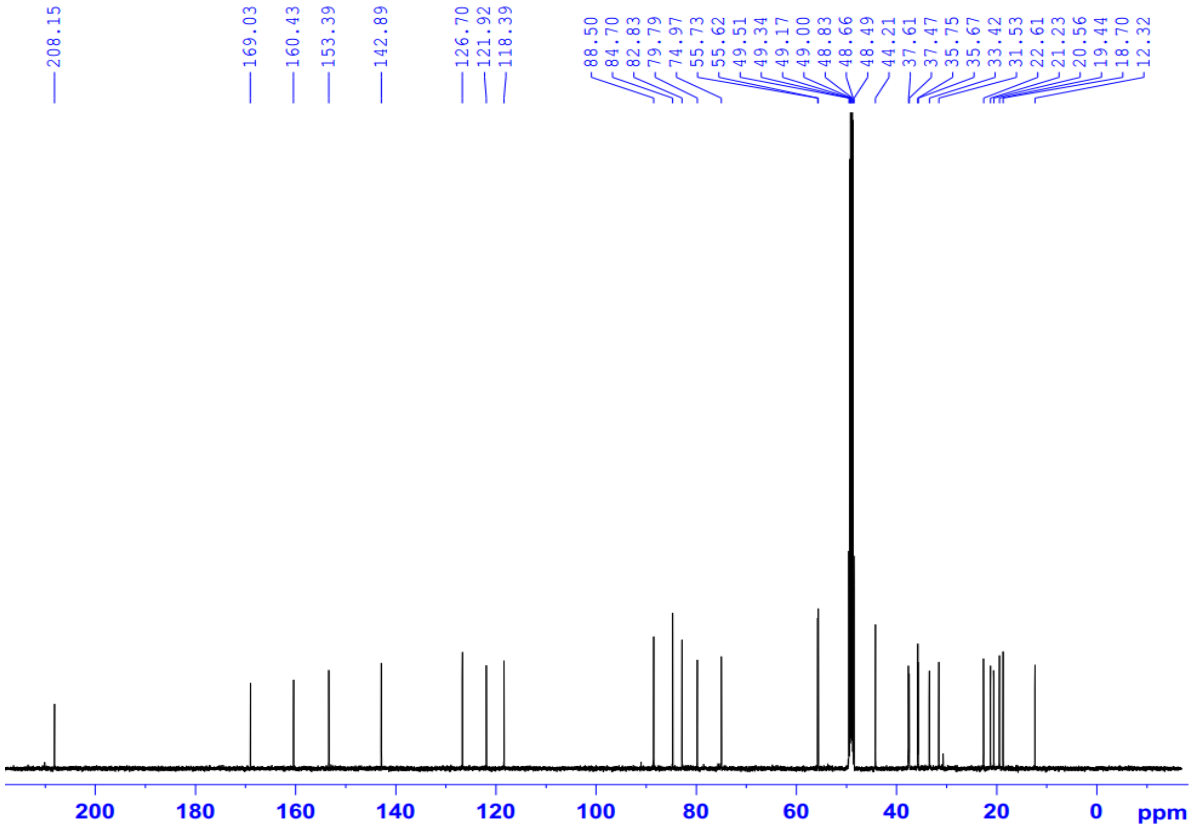

Figure S6. ^{13}C-NMR spectrum (MeOD-d_4, 125 MHz) of compound (**2**)

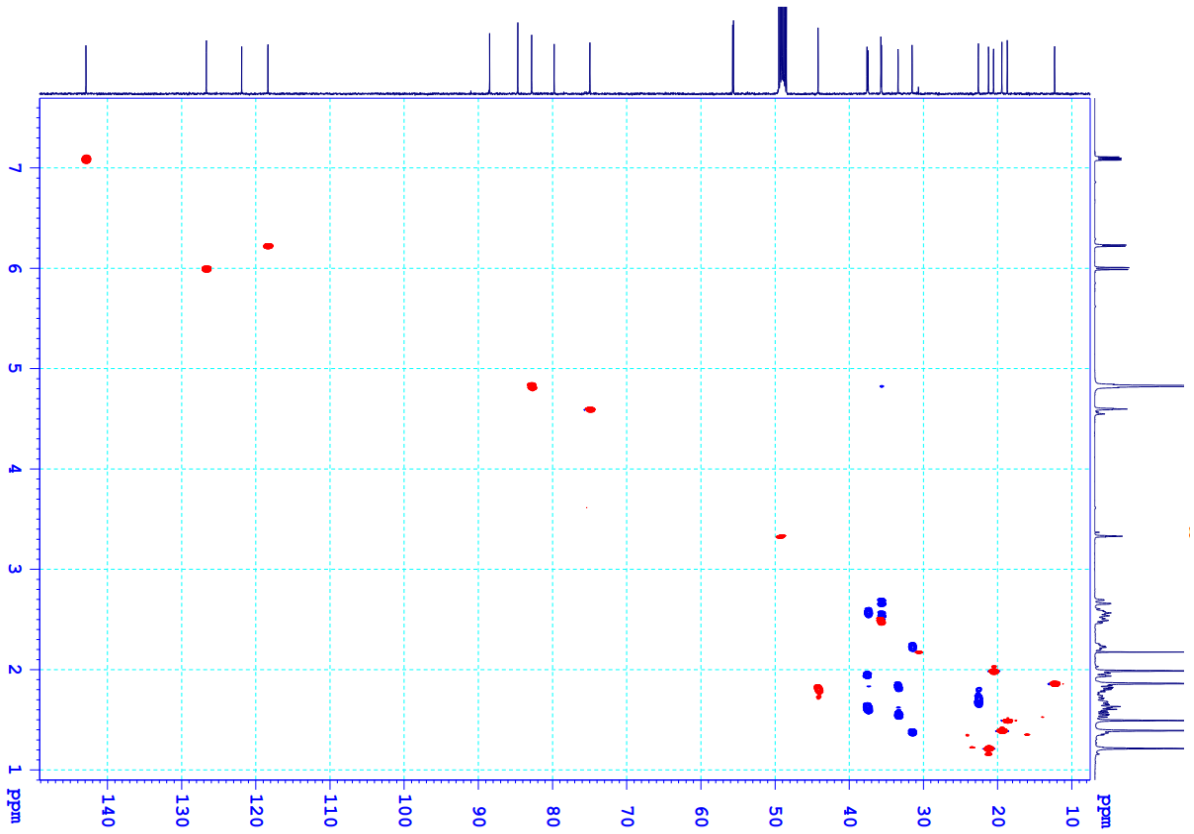

Figure S7. HSQC spectrum of compound (**2**)

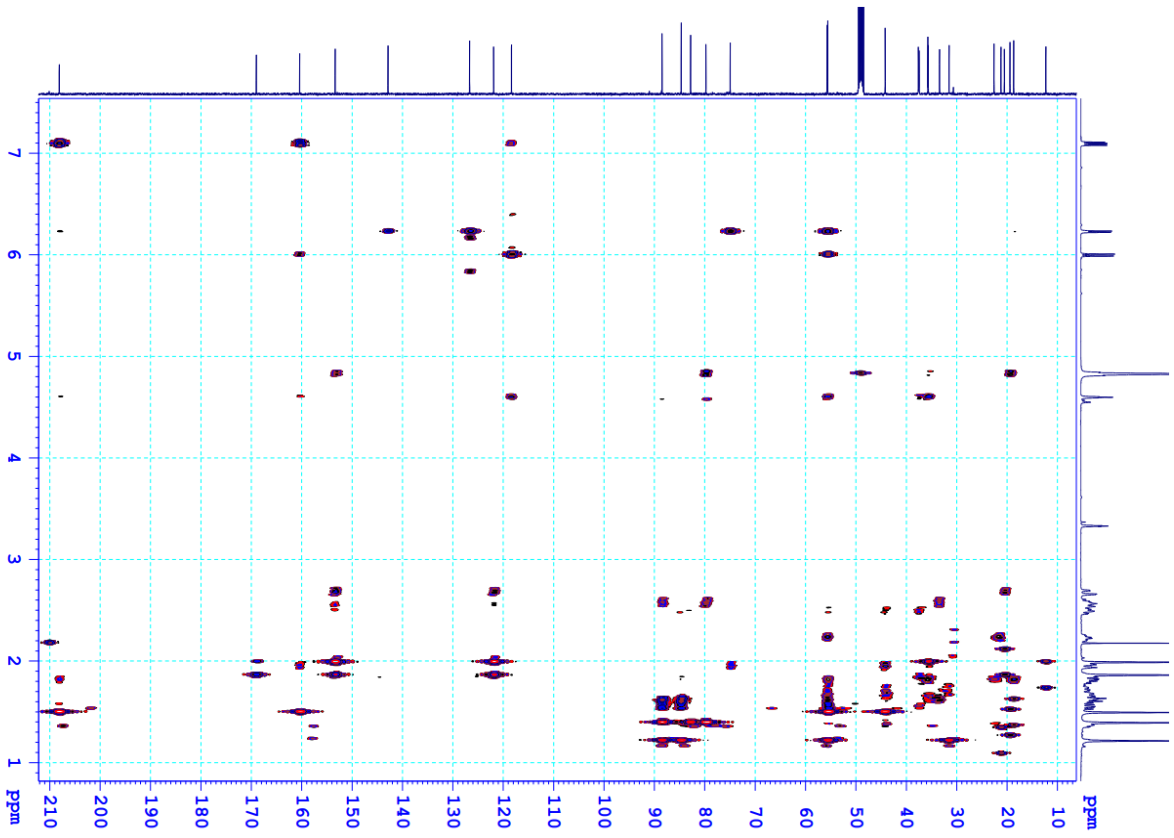

Figure S8. HMBC spectrum of compound (**2**)

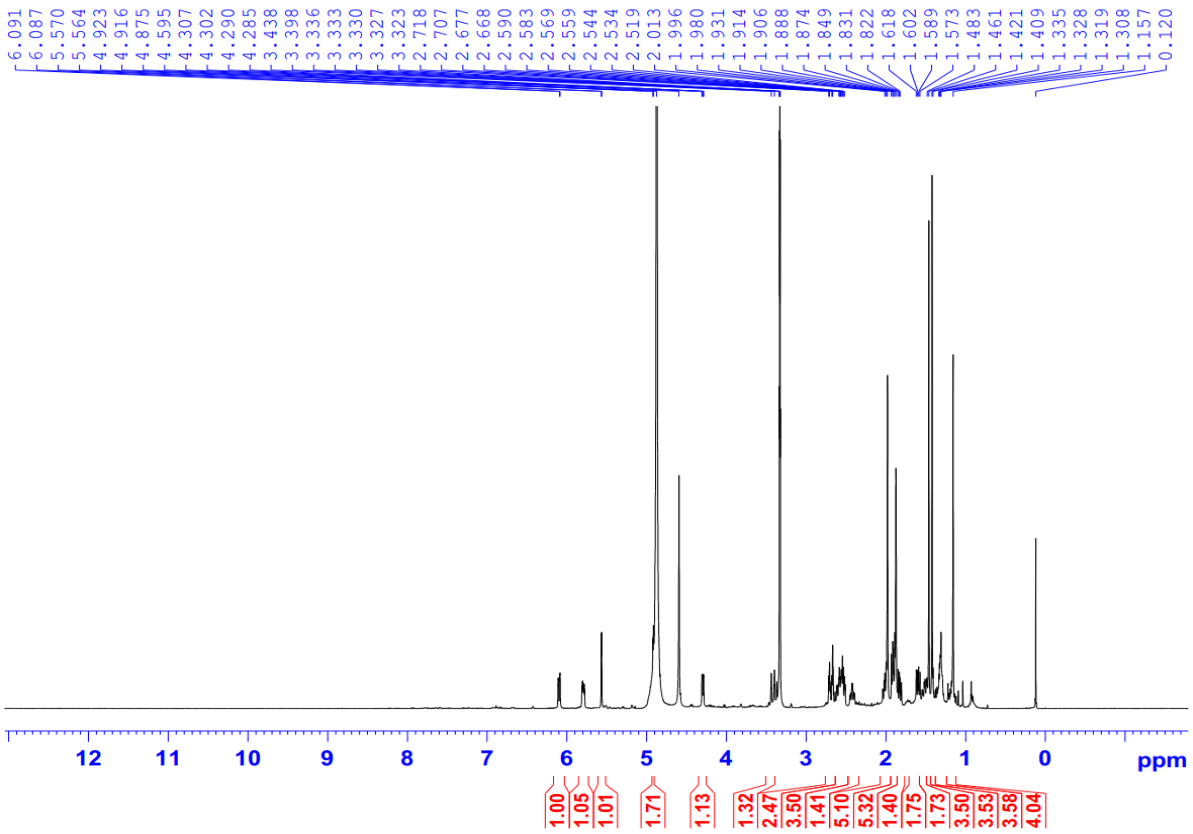

Figure S9. ^{1}H-NMR spectrum (MeOD-d_4, 500 MHz) of compound (**3**)

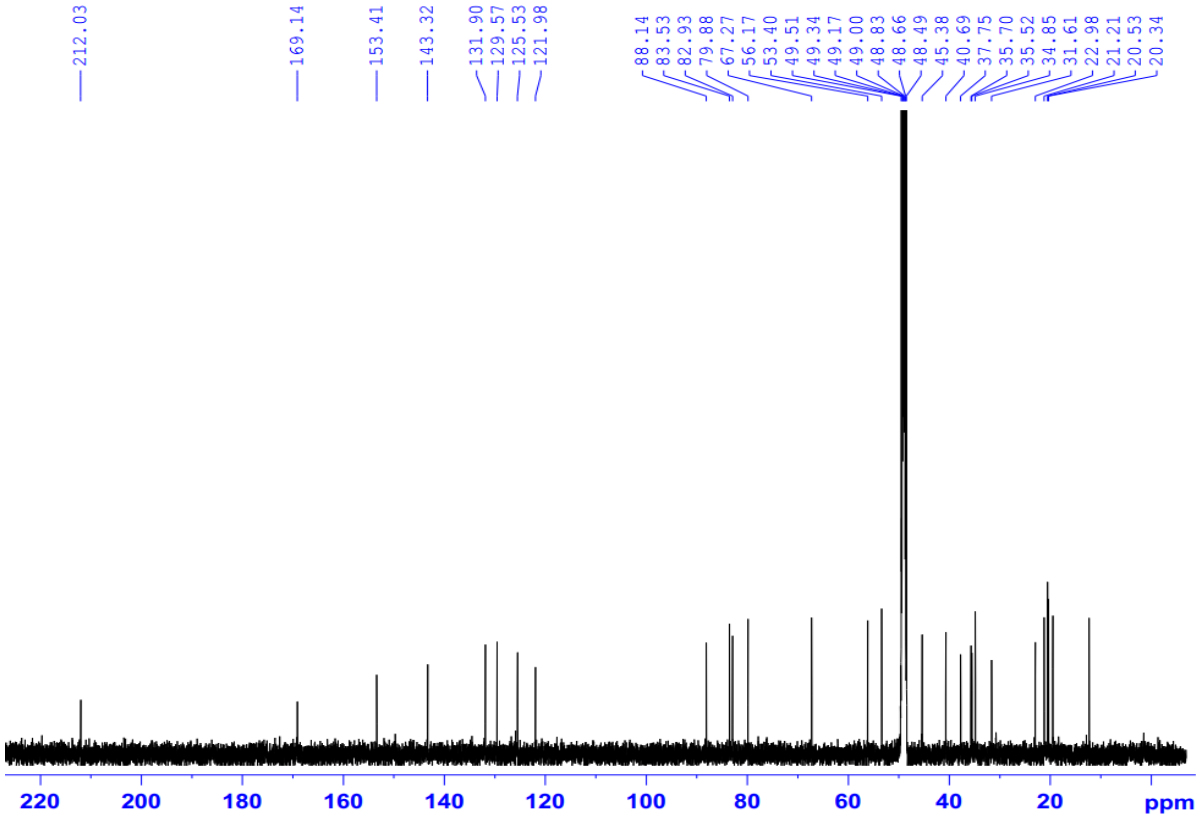

Figure S10. ^{13}C-NMR spectrum (MeOD-d_4, 125 MHz) of compound (**3**)

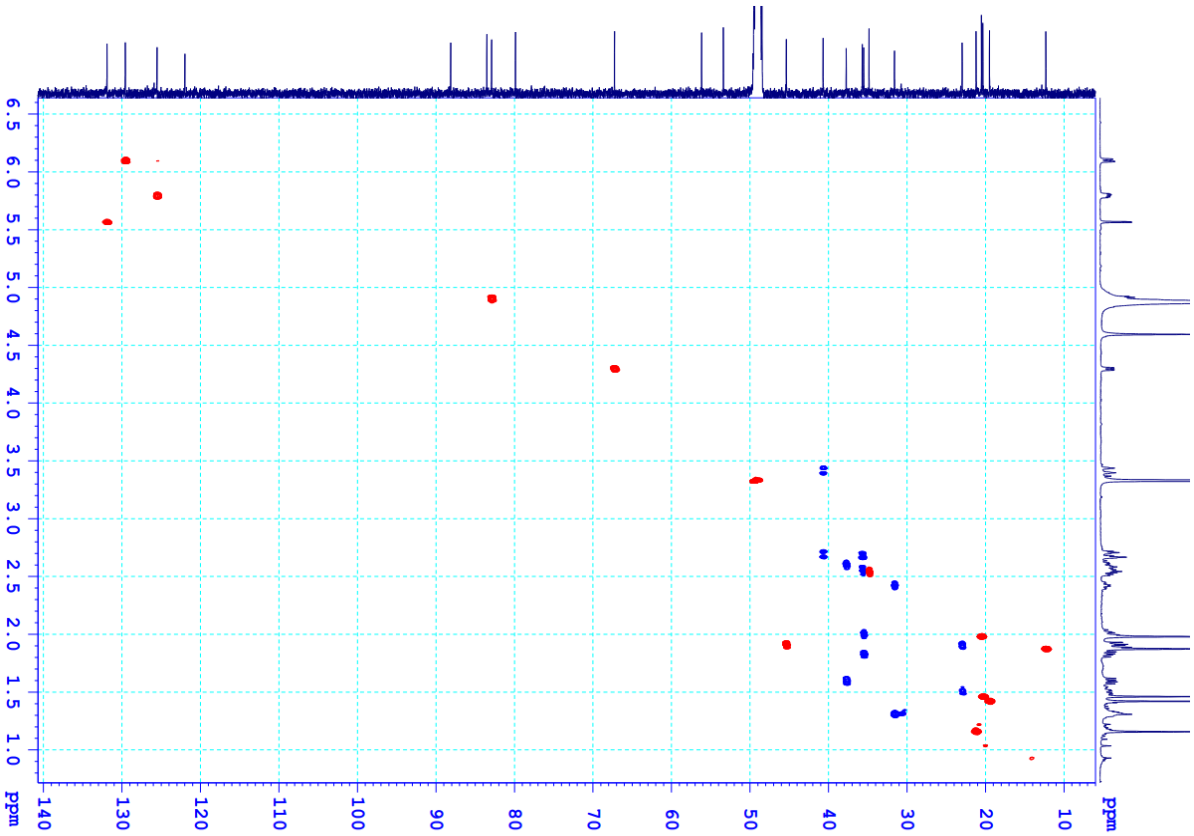

Figure S11. HSQC spectrum of compound (**3**)

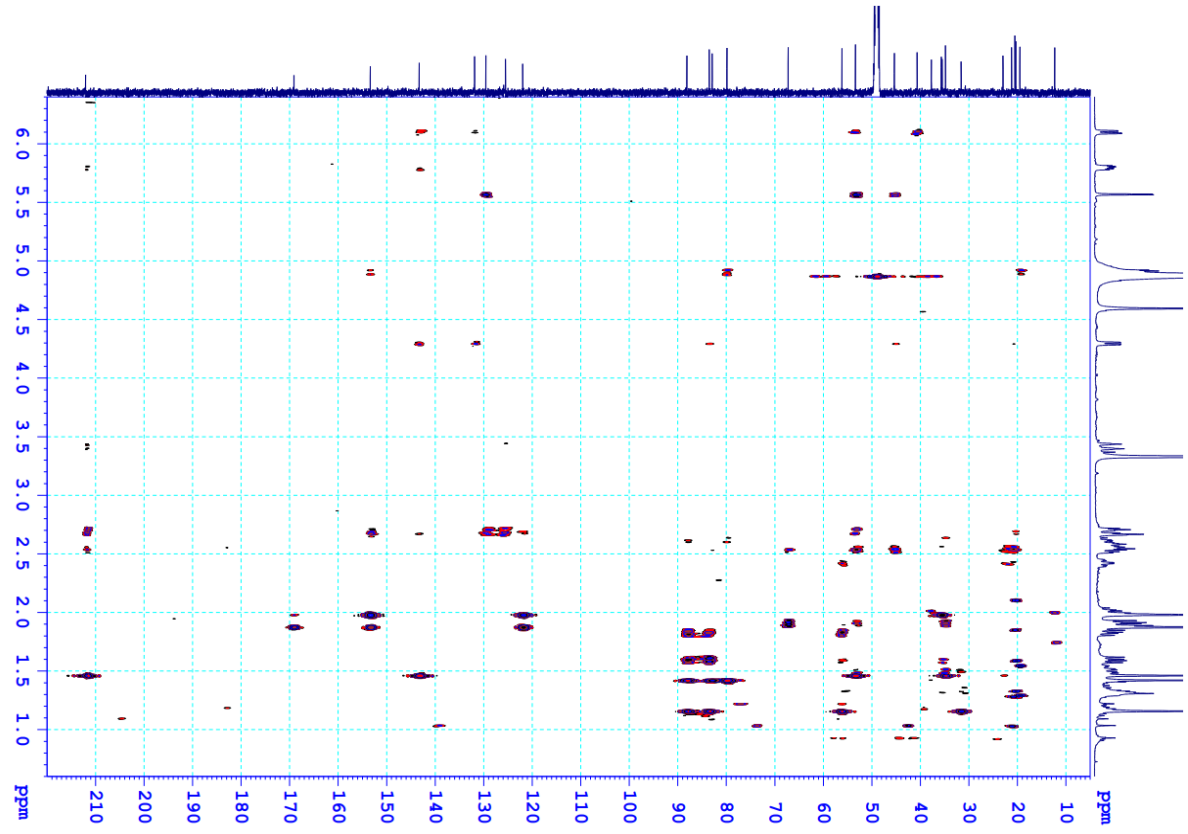

Figure S12. HMBC spectrum of compound (**3**)

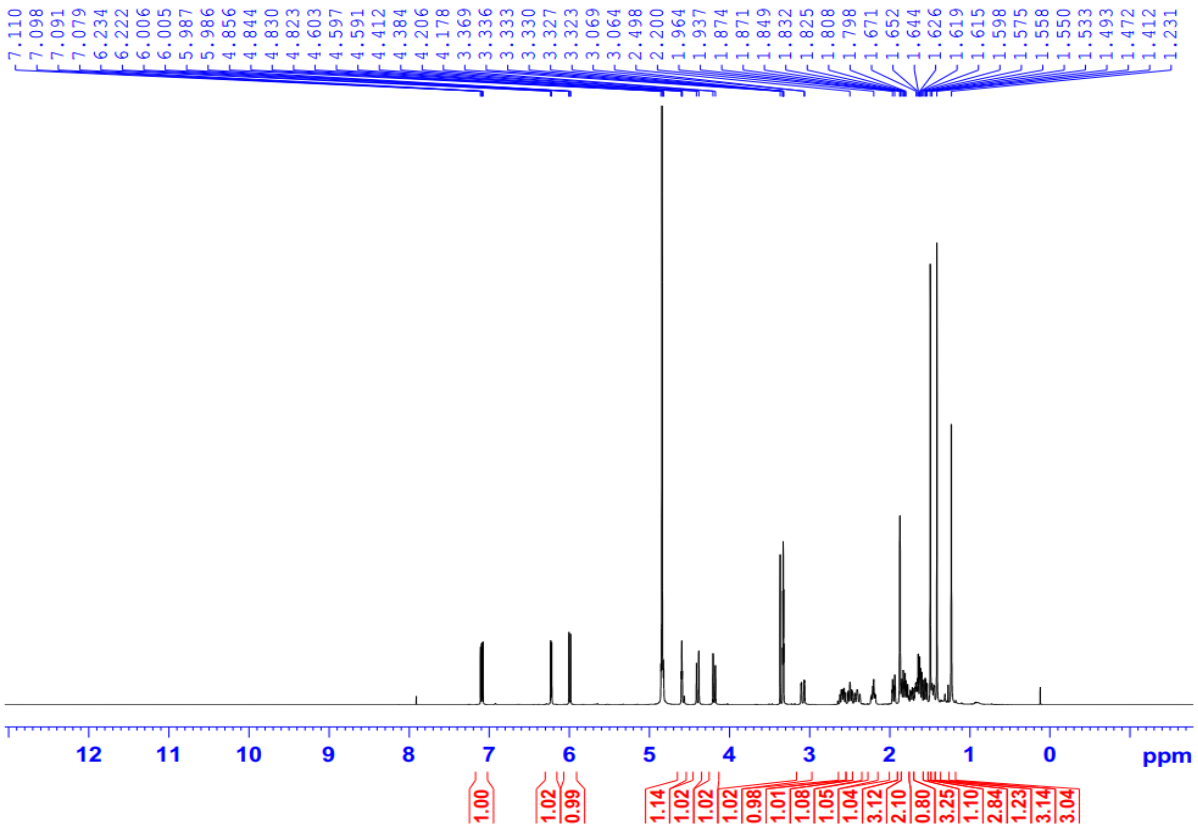

Figure S13. ^{1}H-NMR spectrum (MeOD-d_4, 500 MHz) of compound (**4**)

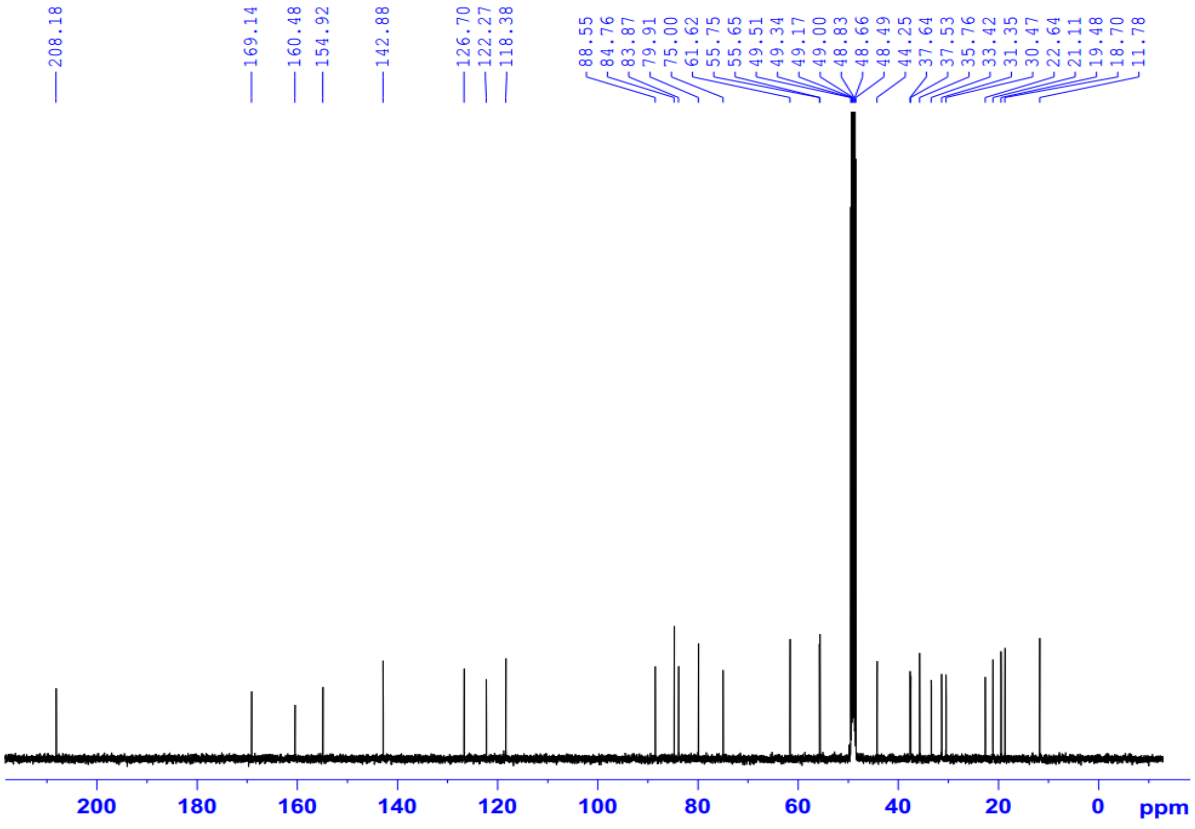

Figure S14. ^{13}C-NMR spectrum (MeOD-d_4, 125 MHz) of compound (**4**)

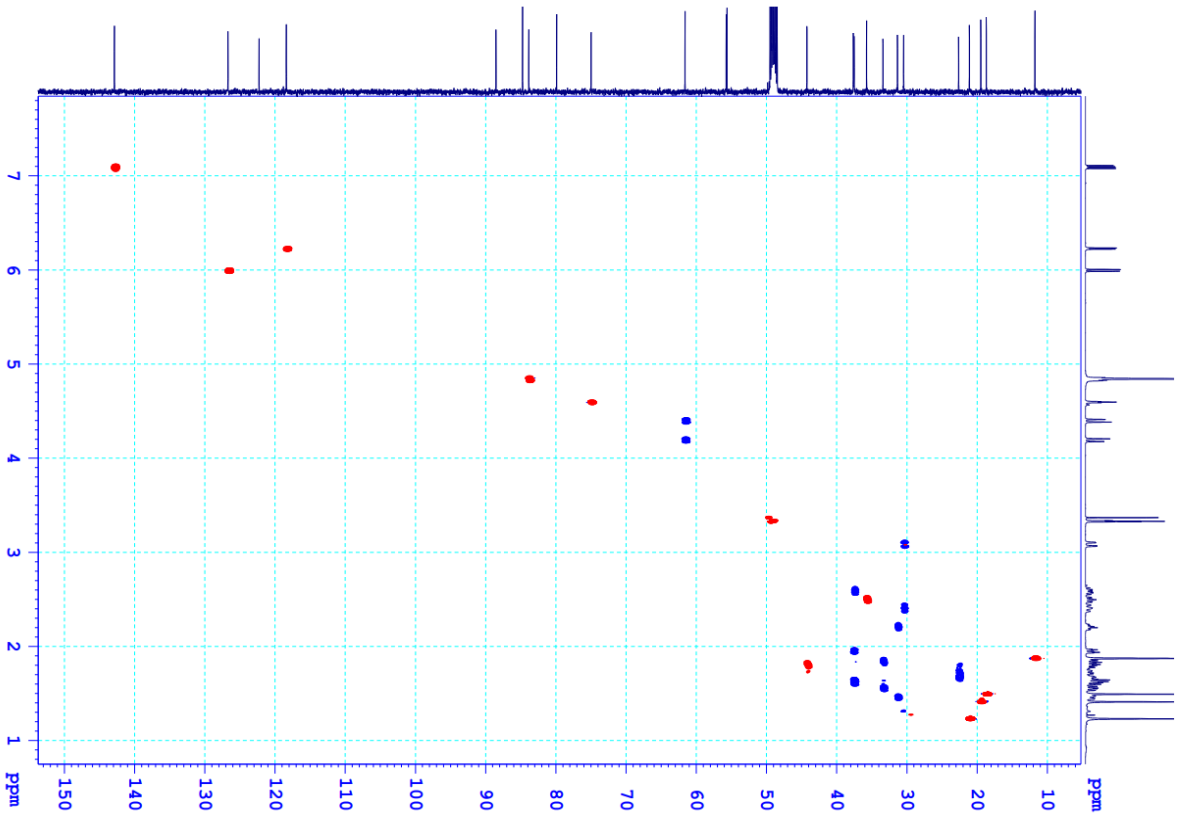

Figure S15. HSQC spectrum of compound (**4**)

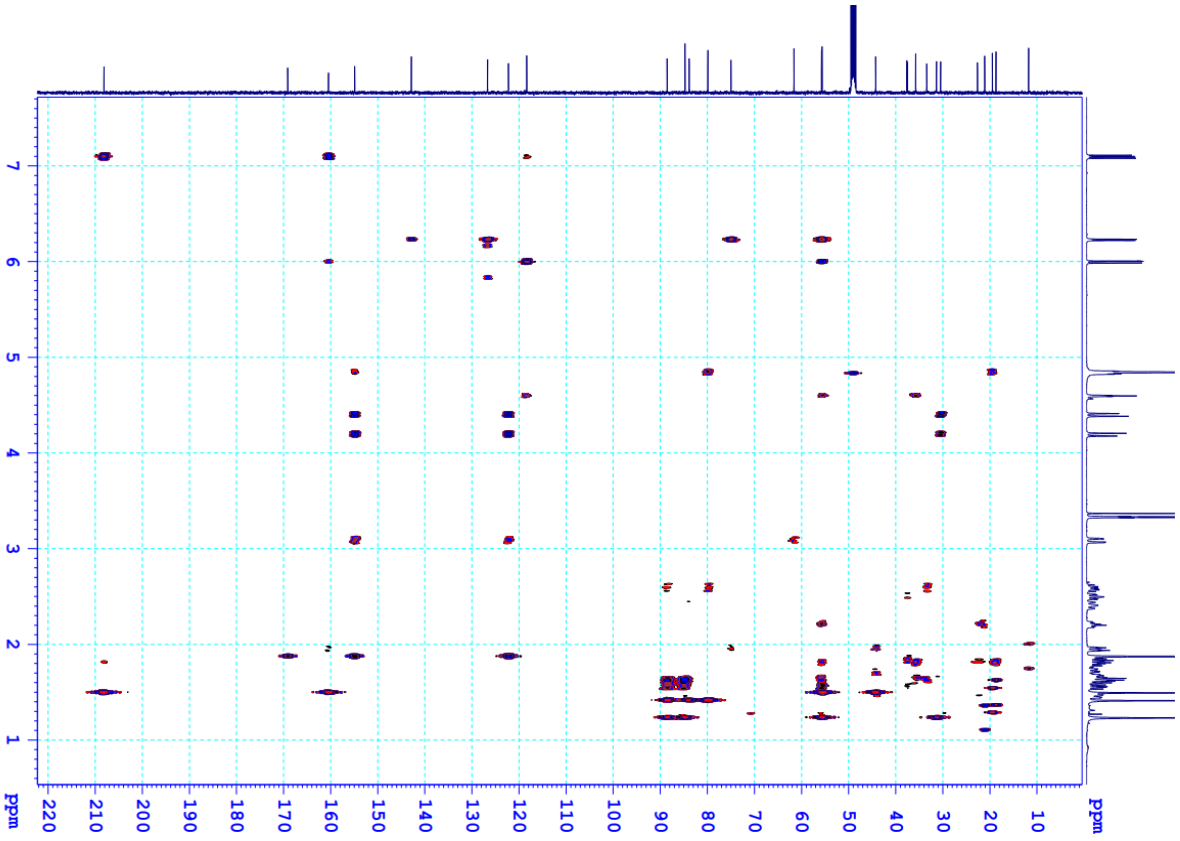

Figure S16. HMBC spectrum of compound (**4**)

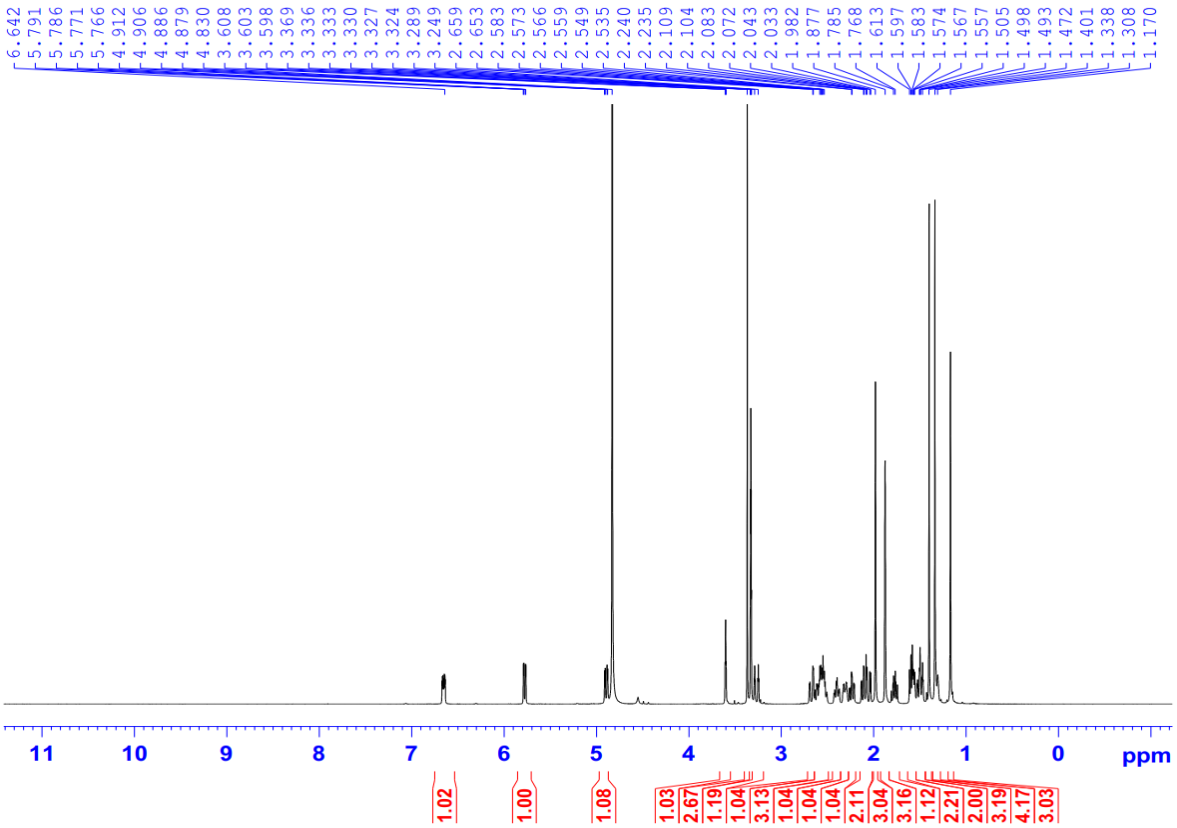

Figure S17. ^{1}H-NMR spectrum (MeOD-d_4, 500 MHz) of compound (**5**)

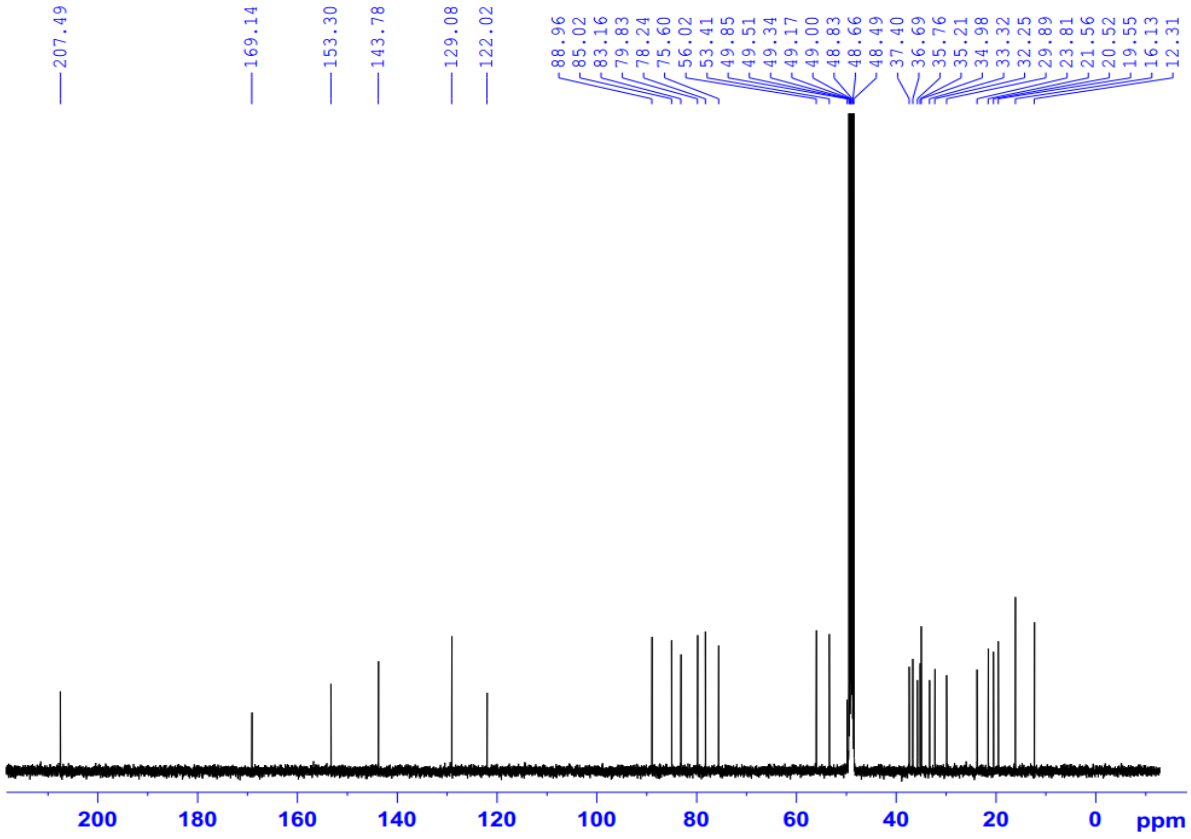

Figure S18. ^{13}C-NMR spectrum (MeOD-d_4, 125 MHz) of compound (**5**)

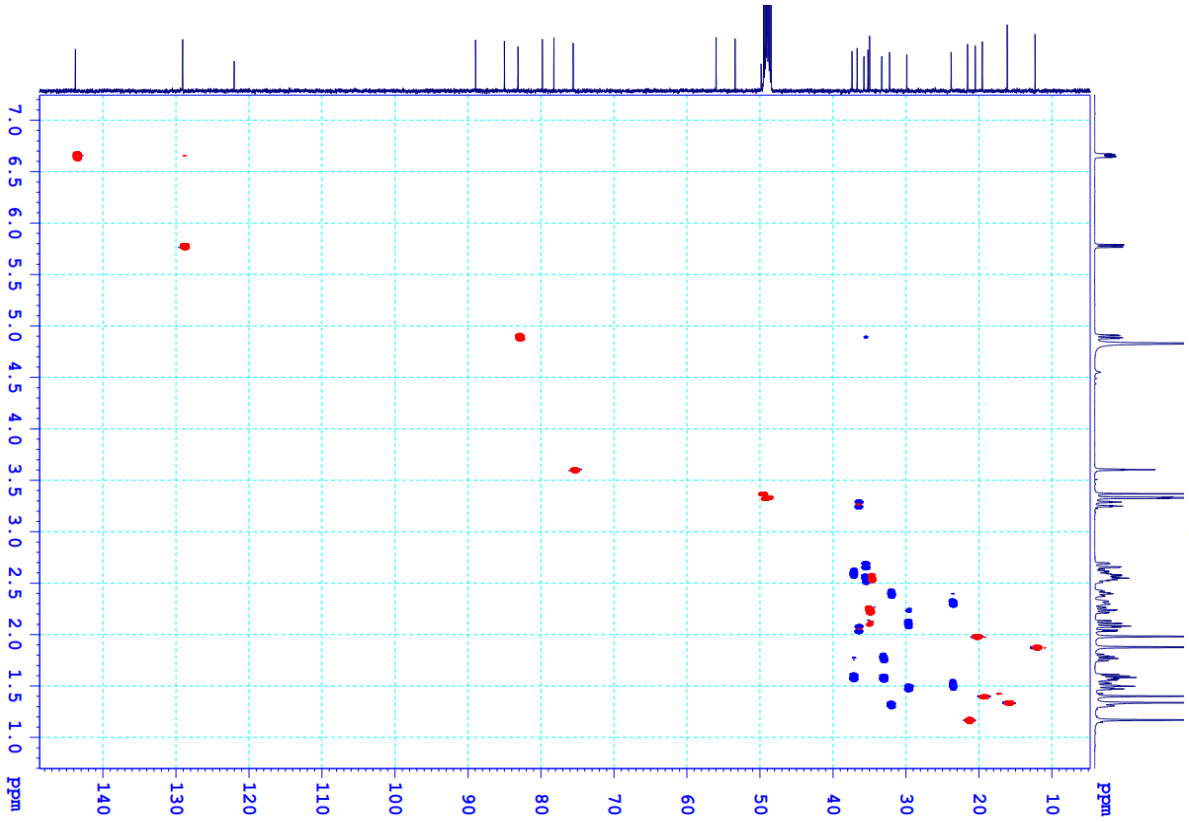

Figure S19. HSQC spectrum of compound (**5**)

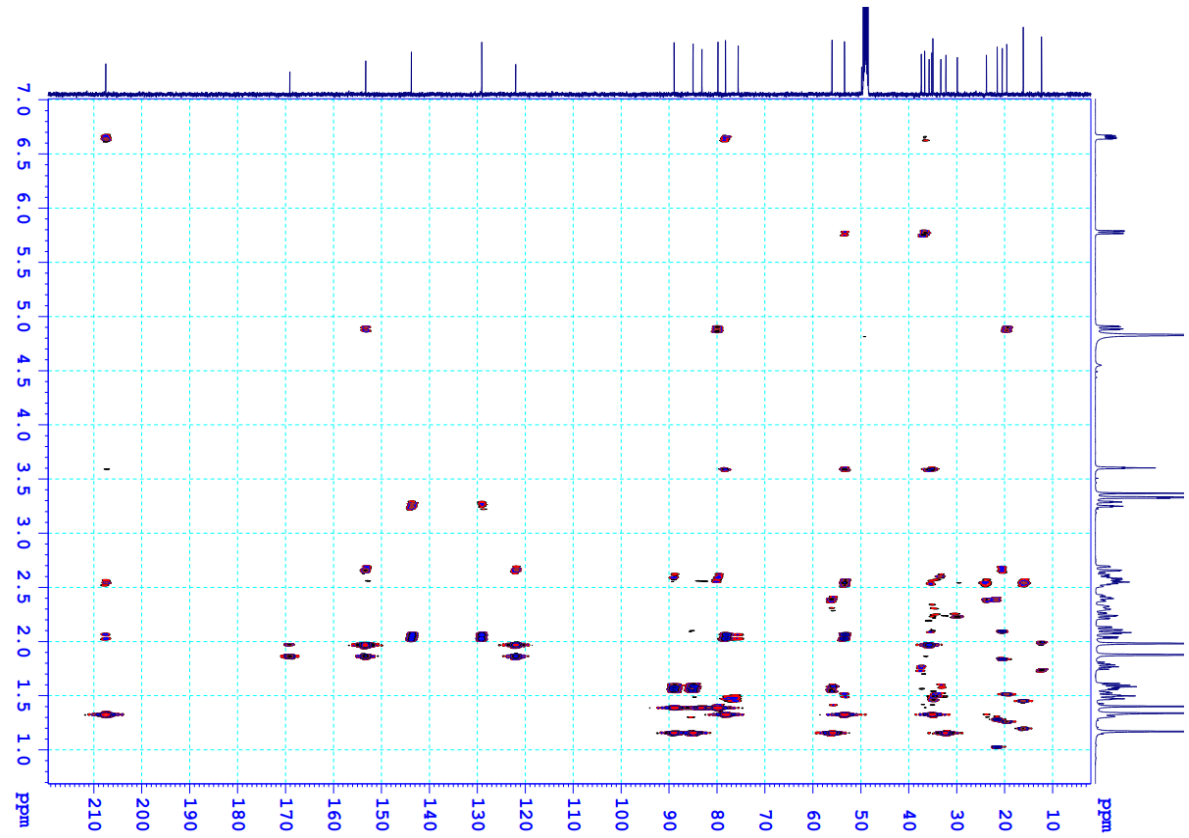

Figure S20. HMBC spectrum of compound (**5**)

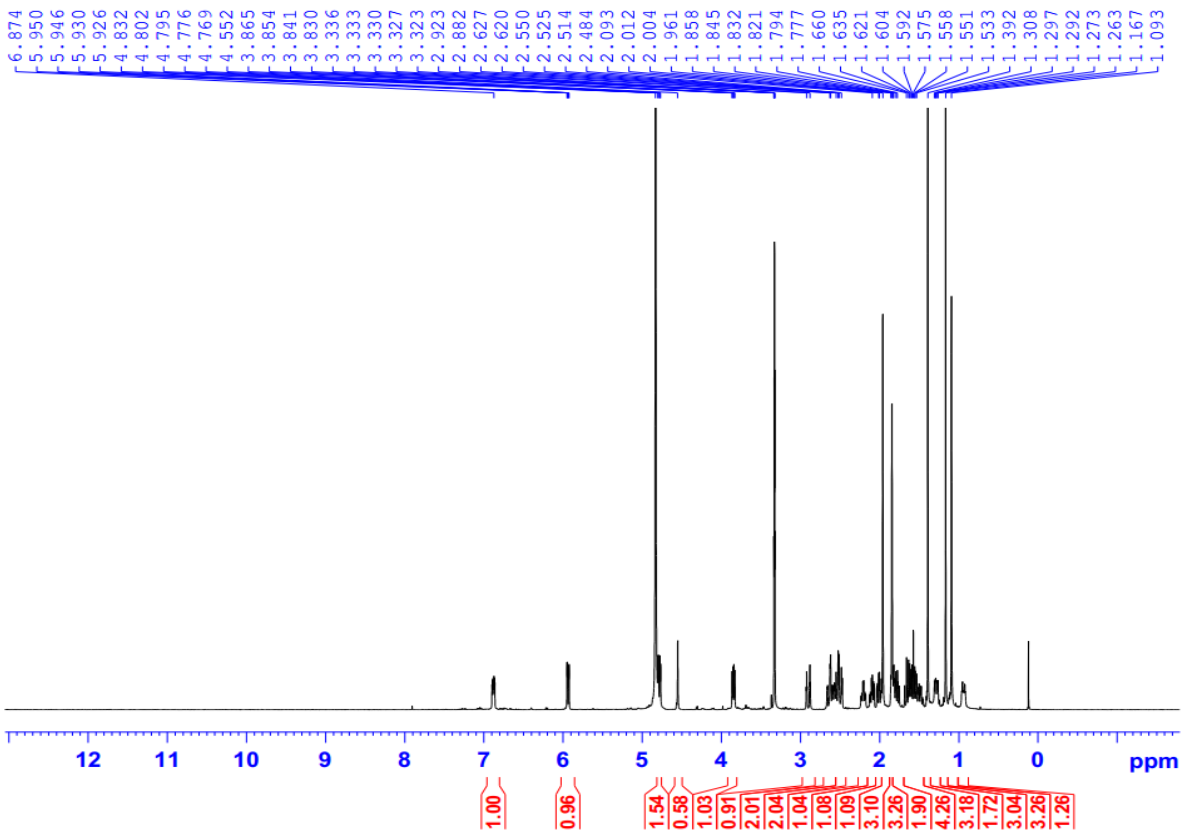

Figure S21. ^{1}H-NMR spectrum (MeOD-d_4, 500 MHz) of compound (**6**)

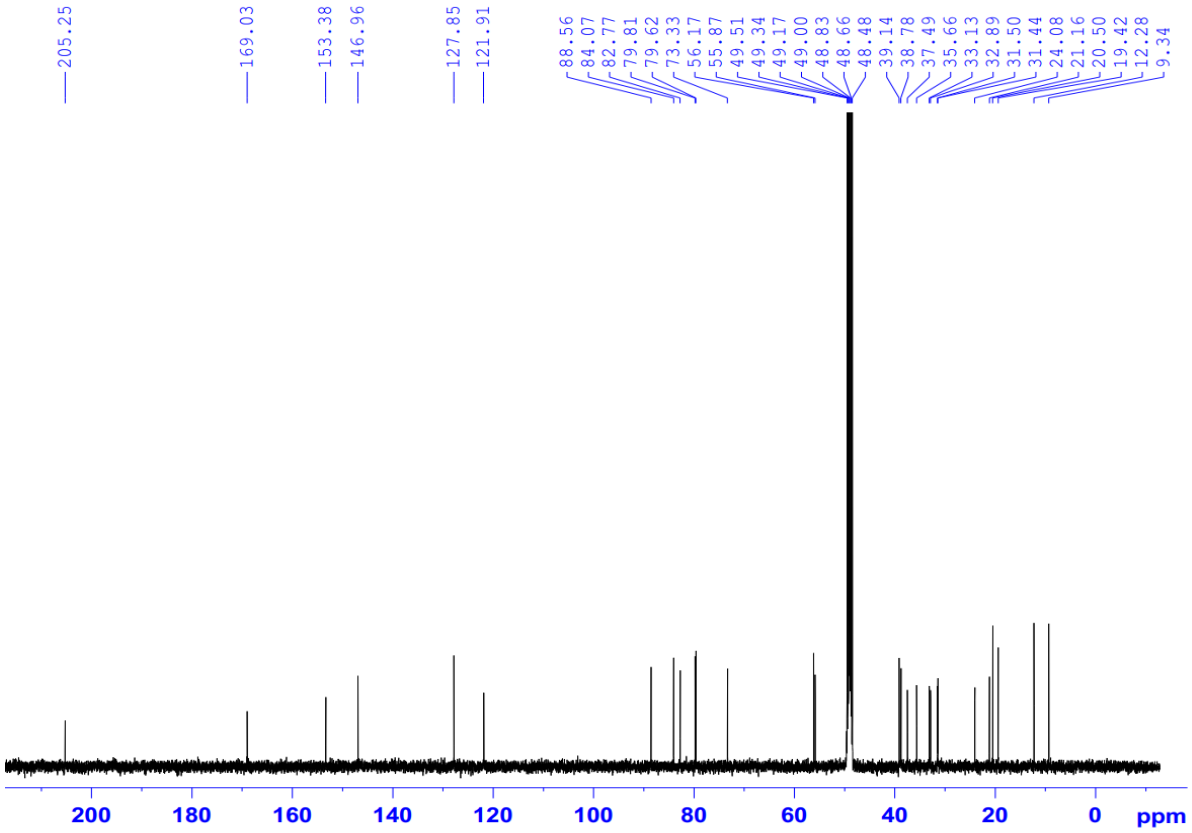

Figure S22. ^{13}C-NMR spectrum (MeOD-d_4, 125 MHz) of compound (**6**)

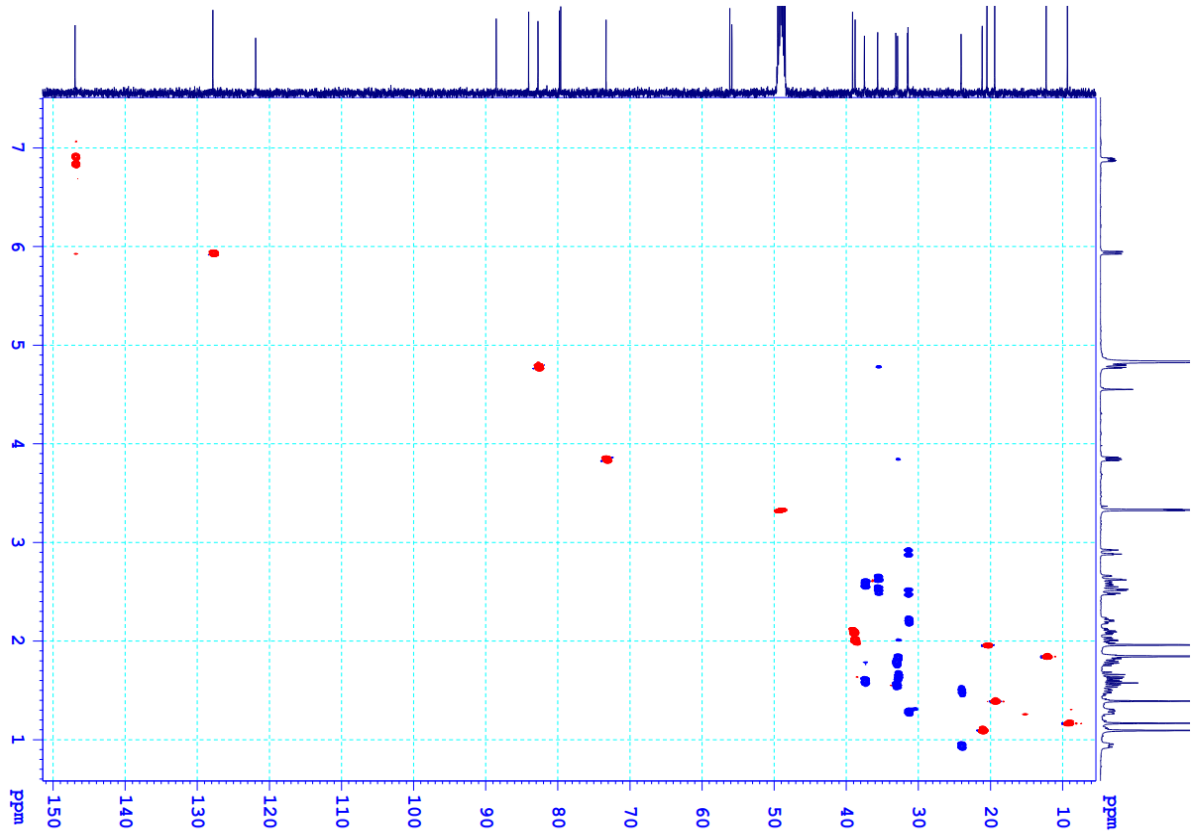

Figure S23. HSQC spectrum of compound (**6**)

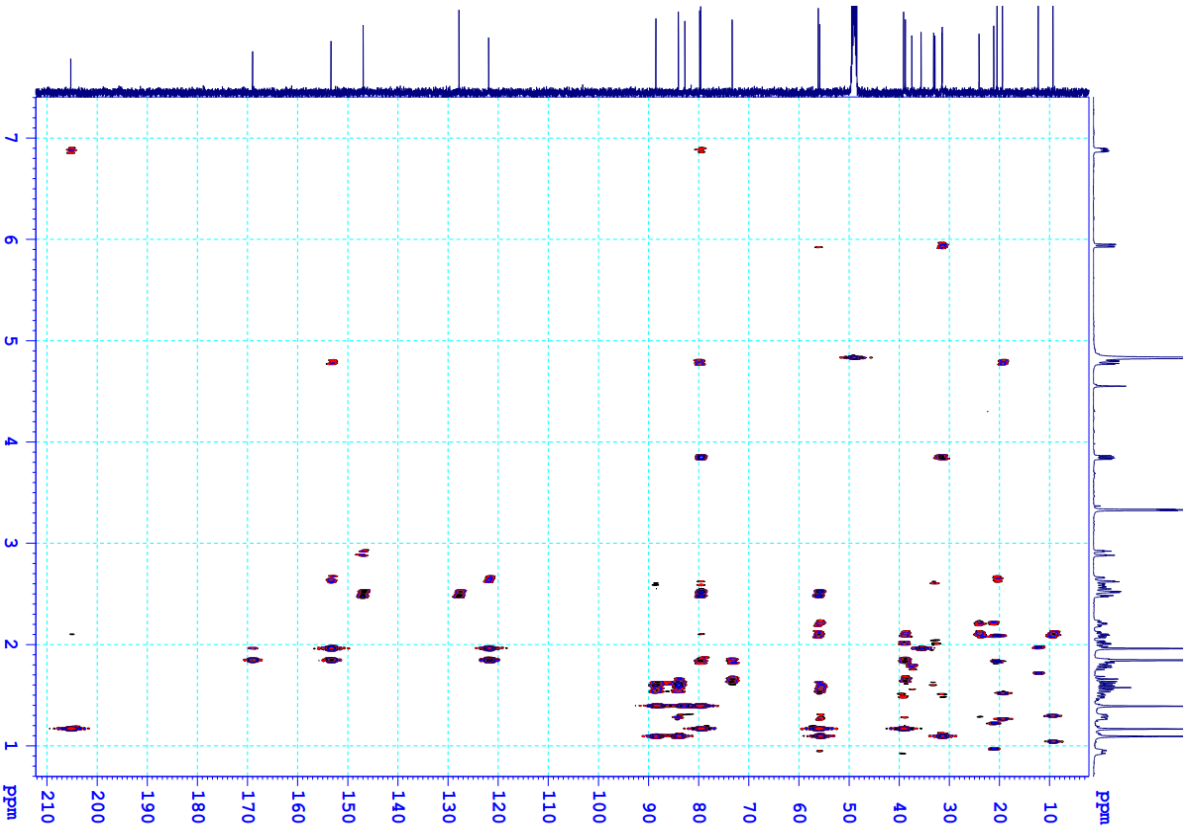

Figure S24. HMBC spectrum of compound (**6**)

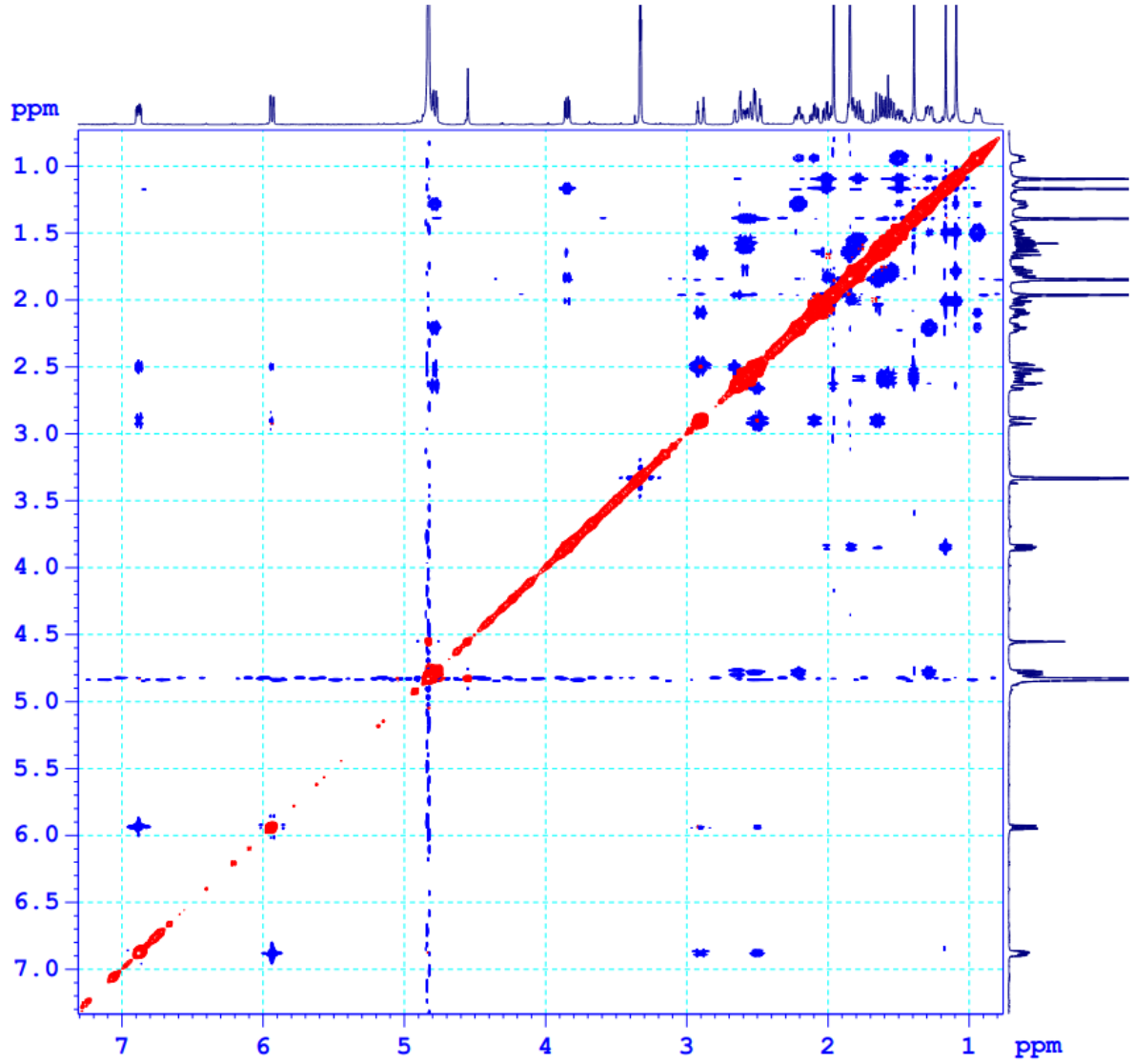

Figure S25. NOESY spectrum of compound (**6**)

Monks A, Scudiero D, Skehan P, Shoemaker R, Paull K, Vistica D, Hose C, Langley J, Cronise P, Vaigro-Wolff A et al. 1991. Feasibility of a high-flux anticancer drug screen using a diverse panel of cultured human tumor cell lines. Journal of the National Cancer Institute. 83(11):757-766. eng.

Shoemaker RH, Scudiero DA, Melillo G, Currens MJ, Monks AP, Rabow AA, Covell DG, Sausville EA. 2002. Application of high-throughput, molecular-targeted screening to anticancer drug discovery. Current topics in medicinal chemistry. 2(3):229-246. eng.